Chapter 1

Application of Radiation Technologies for Quality Improvement of LEDs Based upon AlGaAs

Alexandr V. Gradoboev, Anastasiia V. Simonova,
Ksenia N. Orlova and Olga O. Babich

Additional information is available at the end of the chapter

http://dx.doi.org/10.5772/intechopen.72286

Abstract

The investigation results of the radiation resistance and reliability of light-emitting diodes (LEDs) based upon AlGaAs are presented. The radiation model and the reliability model are described for LEDs. Preliminary irradiation by gamma-quanta and fast neutrons makes it possible to improve the radiation resistance and reliability of the LEDs during further operation. Based on the developed models, radiation technologies are proposed, and the use of which allows increasing the service properties of the LEDs. The suggested technologies can be used for other types of semiconductor devices.

Keywords: light-emitting diodes, AlGaAs, gamma-quanta, neutrons, reliability

1. Introduction

Nowadays infrared wavelength range light-emitting diodes (IR-LEDs) are broadly used in various microelectronic devices that operate in space conditions and at nuclear power plants. Therefore, one already needs to know both their reliability and radiation resistance at the developmental stage. Moreover, operation conditions of LEDs require knowledge of their durability and reliability with complex and combined influence of radiation resistance and long-term operation [1]. In this case, we interpret that complex influence as the simultaneous impact of two or more radiation factors. Accordingly, the combined influence is the impact of two or more radiation factors spread out over a period of time. This is due to the fact that complex and/or combined influence of various types of ionizing radiation is always observed in field operating condition of semiconductor devices. Investigations in this field allow us to develop a radiation model of semiconductor device that describes the changes in its criterial parameters depending on the level and conditions of radiation effect and allows predicting its mode of behavior under the influence. In this case, the criterial parameter of a semiconductor device means such parameter, the change in which limits its working life.

In the same way, the reliability model of semiconductor devices is strictly necessary, which allows to predict the change in criterial parameters during operation.

We should note that it is urgent to add the factors of long-term operation to radiation factors in field operating conditions of the semiconductor devices. Therefore, it is necessary to develop an exploitable model of semiconductor devices [2], which allows describing the change in reliability indexes during long-term operation under conditions of complex and combined influence of various types of ionizing radiation.

At present time, there is an insignificant amount of work on combined influence of ionizing irradiation of semiconductor devices [1, 3–5]. However, works on the combined and complex influence of long-term operation factors and ionizing irradiation are almost completely absent.

Of all the variety of types of ionizing radiation, the research of the influence of irradiation by fast neutrons and gamma-quanta on the changes in the characteristics of various types of semiconductor devices is of primary concern.

Why are these two types of ionizing radiation of special interest? We note that the main effect of neutrons in semiconductor materials is to produce displacement damage. This later can cause shifts in the spectral response, the threshold current, the quantum yield, and the slope efficiency of the LEDs. At that time, ionization mechanism of defect formation dominates for gamma-quanta [6–9]. All other types of ionizing radiation can be represented by means of certain combination of interaction mechanisms of ionizing radiation in terms of their effect on materials. Therefore, the research results of irradiation by fast neutrons and gamma-quanta of various semiconductor device types can be used as a basis for analyzing the influence of other ionizing radiation types and, accordingly, can be used as a basis for developing radiation model of the semiconductor devices.

At the present time, there are no effective and sufficiently reliable methods for calculating the resistance of semiconductor devices to the influence of ionizing irradiation. Therefore, various different simulated equipments are used to determine their resistance to ionizing irradiation [10, 11].

In addition, accelerated tests are generally used to determine reliability indexes of semiconductor devices. They force the aging processes and reduce the length of time required for obtaining the reliability information [12–14]. Generally, the accelerating factors arise from temperature and exaggeration of conditions.

Analysis of the available literature data allows us to conclude that all currently available methods of semiconductor devices' reliability assessment are time-consuming, requiring significant financial expenditures and special equipments. Therefore, obtaining information about reliability and radiation resistance is difficult at the developmental stage of devices.

On the other hand, it is known that ionizing irradiation allows changing directly the parameters of various types of semiconductor devices [1].

The purpose of this work is to develop the radiation technologies focused on improving the reliability of the LEDs based upon AlGaAs heterostructures. The irradiation by fast neutrons and gamma-quanta ^{60}Co is used as a basis of these radiation technologies.

2. Materials and methods

The objects of this investigation were industrial LEDs manufactured on the basis of dual AlGaAs heterostructures with about 2 μm active layer grown on the monocrystalline n^+-GaAs wafer by means of liquid epitaxy. The crystal size was 450 × 450 μm^2. The investigated LEDs have wide application. Ohmic contact to n^+-GaAs has been made on the (Au-Ge-Ni) basis and for AlGaAs layer on the (Au-Zn) basis.

Double heterostructures significantly exceed single heterostructures and bulk materials in terms of their operation parameters. In particular, the n- and p-layers are made from wide bandgap materials except the absorption. Therefore, the wide-gap window effect is observed [15]. In addition, the used n- and p-layers can be heavily doped. Moreover, the injected electrons and holes are in a very narrow active layer, where $n \cdot p$ is extremely high. It increases the rate of radiative recombination [16]. In addition, LEDs based upon double AlGaAs heterostructures have a higher resistance to ionizing radiation [17, 18]. The above advantages are the main reasons for choosing the object of research.

Figure 1 represents the structure of the double AlGaAs heterostructure of the LED. In the left part of **Figure 1**, the layers of semiconductor materials are shown (the doping impurity is indicated in parentheses). Furthermore, the thickness of the layers is given in the central part of **Figure 1**. Moreover, the distribution profile of the concentration of the main charge carriers and the Al content in the layers are shown on the right part of **Figure 1**.

LEDs were manufactured using standard sandwich technology that involves metallic layer deposition and shaping processes for ohmic contact creation, photolithographic and chemical etching processes for die formation, and dicing for wafer division into individual chips. LEDs had packages and lenses made of an optical compound that was used to form the required angular pattern for output lumen. We emphasize that the preliminary investigation shows us that optical compound irradiation by fast neutrons, and gamma-quanta do not lead to changing its optical properties in given wavelength range. Consequently, we suggest that the changing of the observable light characteristics of the LEDs is due to the changing of characteristics in their active layer only.

In continuous power mode, the LED forward operating current was I_{op1} = 50 mA, and supply voltage U_{op} was not over U_{op} = 2.0 V. The maximum emissive wavelength was within the range of 0.82–0.90 μm. Emissive power at the given operating current was criterial parameter of the LEDs that determined their efficiency.

For every LED emissive power at operating current 50 mA under normal conditions was taken using a measurement complex with spherical photometric integrator. The error did not exceed 5% of emissive power measurement of LEDs. The spread of the emissive power of the initial LEDs for each batch did not exceed ±10%. Moreover, the spread of the operating voltage was ±3%.

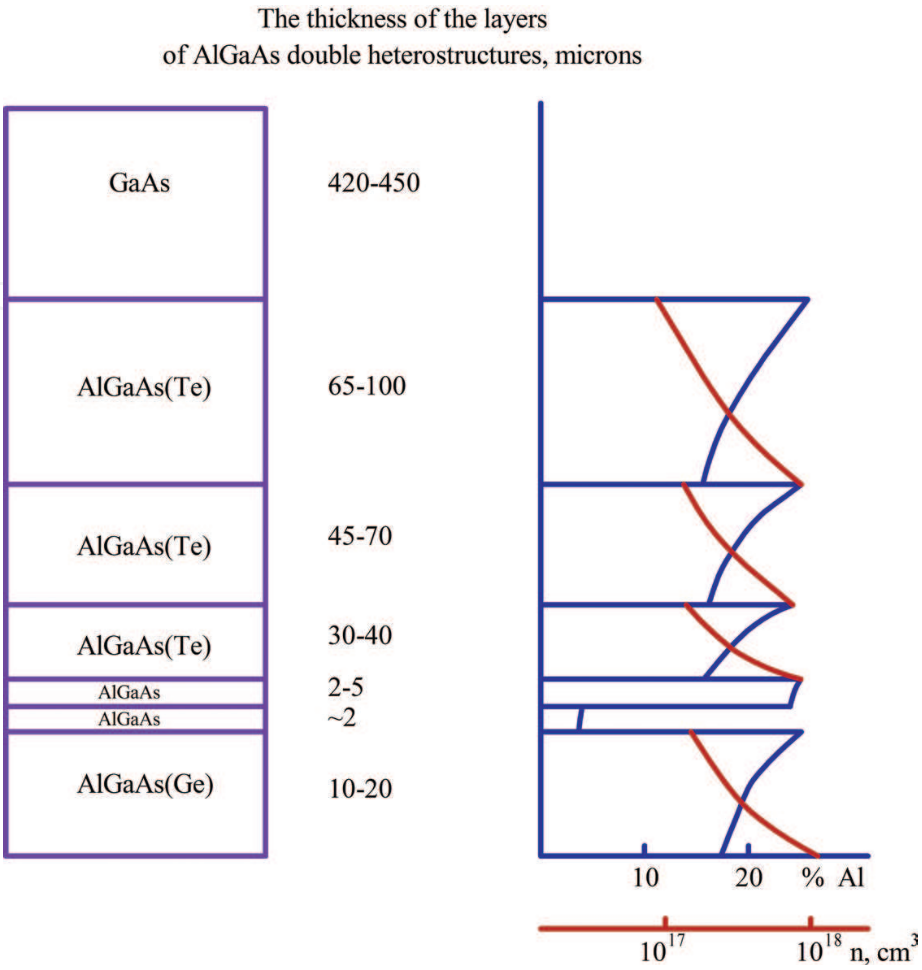

Figure 1. Structure of the double AlGaAs heterostructure.

The named characteristic of LEDs was obtained at the very beginning and after every stage of the investigation. The results were processed by means of mathematical statistics methods. Every batch of LEDs under investigation was characterized by average values of measured parameters.

Irradiation by gamma-quanta was performed with isotopic continuous source of ^{60}Co. The exposure level was characterized by the absorbed dose D_γ [Gy]. The dose rate was about 1 Gy/s, and the average gamma-quanta energy was 1.25 MeV.

Irradiation by fast neutrons was carried out on the pulse simulator installation "Bars-4," which has got a reactor core of the metallic uranium and molybdenum alloy (10% by weight) with a pulse duration of 60 μs. The average neutron energy is 1.4 MeV [19, 20]. The exposure level was characterized by neutron fluence F_n [n/cm^2].

Irradiation by gamma-quanta and fast neutrons was realized in passive power mode, i.e., without the adding external electric field. Moreover, electrical lead of the LEDs was not allowing the flow of electricity.

Long-term operation was modeled using step-by-step tests. Standard certified equipment was used for experiments, and baseplate temperature was 65°C; the increment step of current was ΔI = +50 mA. Operating current of the first stage was I_{op1} = 50 mA. Duration of each stage was t = 24 h. Every stage of testing was characterized by operating current I_{stepi}. Moreover, each stage of the experiments was distinguished by the temperature of the LED active layer T_{stepi}, which depends on ambient temperature (i.e., baseplate temperature) T_0, LEDs thermal resistance R_T, and consumed electric power on *i* step U_{stepi}. Therefore, temperature of the LED active layer on each stage of the tests is determined by the following equation:

$$T_{stepi} = T_0 + R_T + I_{stepi} \times U_{stepi}. \quad (1)$$

Therefore, we used both temperature and operating current as acceleration factors during step-by-step tests. Furthermore, limit step of the tests did not go beyond catastrophic failure (CF) development [21, 22]. The step-by-step tests were stopped when at least 80% of the LEDs were out of service in each batch of the research LEDs.

The following batches of the LEDs were composed for the research. The quantity of the LEDs in each batch was 20 items:

- LED-1 and LED-2 were for resistance research of irradiation by gamma-quanta and fast neutrons.
- LED-3 was for research of reliability.
- LED-4 and LED-5 were for research of influence of preliminary irradiation by gamma-quanta with further annealing on reliability.
- LED-6 and LED-7 were for research of influence of preliminary irradiation by fast neutrons with further annealing on reliability.

Rationale selection of preliminary irradiation level by gamma-quanta and fast neutrons, and annealing parameters will be considered below.

3. Radiation resistance and reliability of the LEDs

3.1. Radiation resistance of the LEDs

Consider the results of a study of the resistance of batch LED-1 to ionizing irradiation. **Figure 2** shows the relative change of emissive power measured at the operating current depending on the absorbed dose of gamma-quanta [23]. Here and further, emissive power *P* measured after exposure is normalized to its initial value P_0 of LEDs. The absorbed doses of $D_{\gamma 1}$ and $D_{\gamma 2}$ in **Figure 2** are explained below in the text.

Whereas **Figure 3** depicts the relative change of emissive power of the batch LED-2 measured at the operating current depending on fluence of fast neutrons [24]. The fluences F_{n1} and F_{n2} in **Figure 3** are explained below in the text.

We note that the spread of emissive power of LEDs in the batch rises to ±15% of average value in the batch when dose of irradiation by gamma-quanta and fluence of fast neutrons increase. Accordingly, the spread of operating voltage of the LEDs rises to ±5%.

These research results suggest the following radiation model of the LEDs. It describes the changes of emissive power of the LEDs under irradiation by gamma-quanta and fast neutrons:

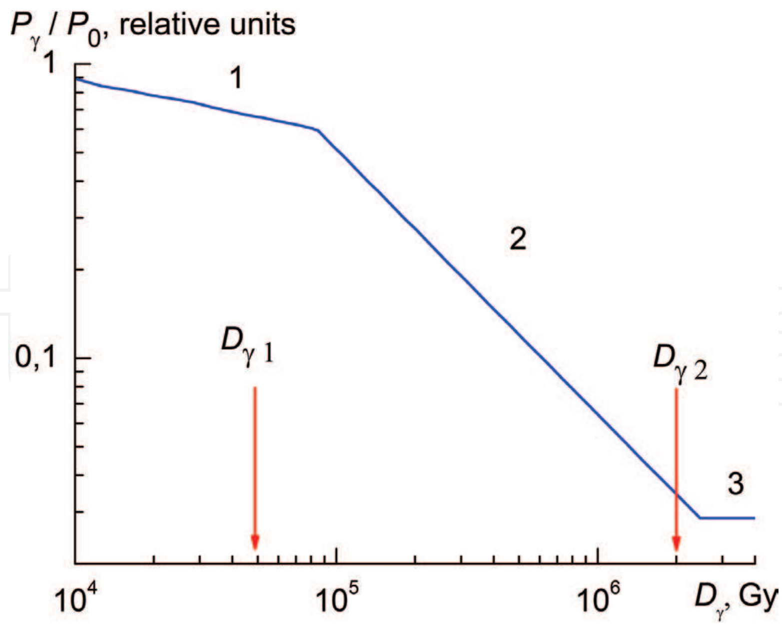

Figure 2. Relative decrease of the emissive power of the LEDs depending on gamma-quanta irradiation dose: 1, 2, and 3, stages of the emissive power decrease; $D_{\gamma 1} = 5 \cdot 10^4$ Gy; $D_{\gamma 2} = 2 \cdot 10^6$Gy.

- In the first stage, the fall of emissive power of the LEDs is attributed to the radiation-stimulated reconstruction of the initial defect structure of the LED crystal (field 1 in **Figures 2** and **3**) as evidenced by saturation of this stage as the level of exposure increases.
- In the second stage, the fall of emissive power of the LEDs during irradiation is attributed solely to the introduction of radiation defects (field 2 in **Figures 2** and **3**).
- In the third stage, the LED transits into the field of low electron injection into the active layer of the LED (field 3 in **Figures 2** and **3**).

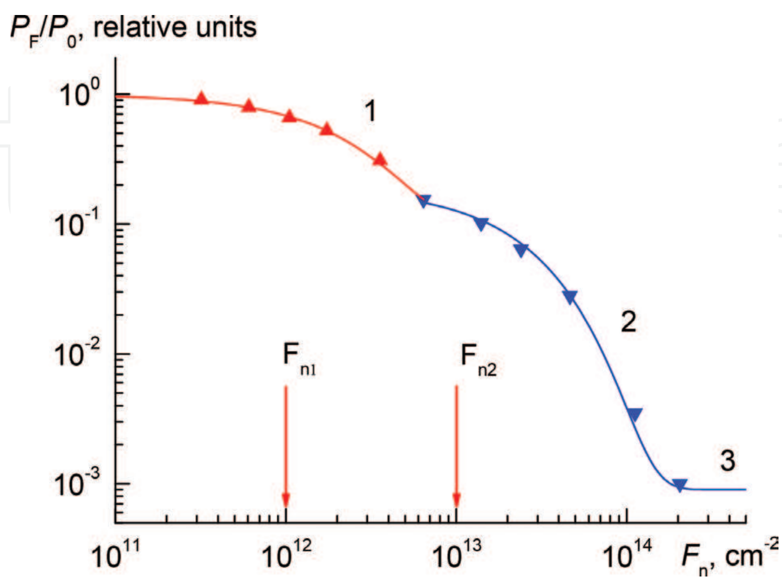

Figure 3. Relative decrease of the emissive power of the LEDs depending on fast neutron fluence: 1, 2, and 3, stages of the emissive power decrease; $F_{n1} = 10^{12}$ n/cm^2; $F_{n2} = 10^{13}$ n/cm^2.

We note that the low electron injection mode is characterized by weak dependence of emissive power of the LEDs on operating current value [25].

It should be particularly emphasized that in the third stage, the CF is observed and caused by accelerated degradation of ohmic contacts' "metal semiconductor" [22, 26].

Additionally, the type of the ionizing radiation determines the relative contribution of the first stage of the emissive power decrease of the LEDs, which is due to the influence of the type of ionizing radiation on the efficiency of the reconstruction of the initial defect structure. We compared the experimental results presented in **Figures 2** and **3**. Therefore, under irradiation by gamma-quanta, the contribution of the first stage of the emissive power decrease of LEDs is about 40% of the initial emissive power, while for fast neutrons, it is about 85%.

This radiation model of the LEDs completely corresponds to previously discussed model of LEDs based on other materials [27–29]. Therefore, the radiation model of decrease of emissive power of the LEDs can be extended to practically all LEDs made of various semiconductor materials.

Each of the named distinctive stages of the emissive power fall of the LEDs under irradiation can be described by the corresponding empirical relationships with their own damage constants. They are usually used to describe the processes of changing the criterial parameters of devices under various influences [30, 31]. The established relationships are capable of predicting the radiation resistance of the LEDs.

3.2. Reliability of the LEDs

Next, consider the changes of emissive power during operation and more specifically during step-by-step tests. **Figure 4** presents relative change of emissive power of the batch LED-3 during step-by-step tests.

Decrease of emissive power during step-by-step tests can be characterized by three distinctive stages, which we observed previously while investigating the radiation resistance of the LEDs (part 3.1, **Figures 2** and **3**). One might assume that the first stage of step-by-step tests decrease in LED emissive power (field 1, **Figure 4**) is possible due to rearrangement of original defect structure exposed to long-term operation factors. Accordingly, emissive power gets reduced on the second stage as the result of inducing new structural defects under influence of long-term operation factors (field 2, **Figure 4**). On the third stage of emissive power fall during long-term operation (field 3, **Figure 4**), we can observe a transition into the mode of low electron injection with further origination of CF. We note that degradation of ohmic contacts' "metal semiconductor" is a preliminary to CF during step-by-step tests [22, 26].

The identity of determined stages of the emissive power decrease of the LEDs under influence of ionizing radiation and long-term operation factors allows for the conclusion that the long-term operation factors correspond to the radiation factors according to their physical nature. In this case, one may talk of one whole model of the emissive power degradation of the LEDs due to the influence of ionizing radiation and long-term operation factors. At the same time, it should be specially noted that proper correlations between the established stages are observed for each of these factors. In actual fact, the contribution of

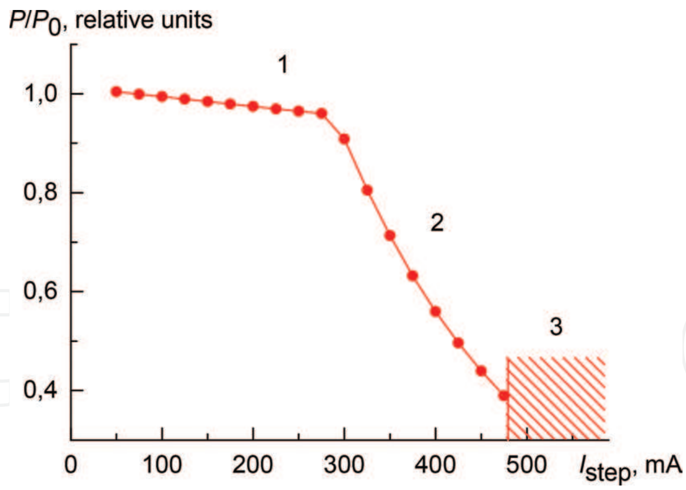

Figure 4. Relative change of the emissive power of the LEDs depending on step number of the tests: 1, 2, and 3, stages of the emissive power decrease.

each determined stages to the overall decrease of the emissive power depends on type of influencing factors. In addition, each stage is characterized by its own value of the damage constants for each type of influencing factors.

The above-presented results have proved the identity of degradation processes in LEDs under the influence of ionizing radiation and factors of long operating time. Therefore, it has been established that under the influence of ionizing radiation on the LED and long-term operation factors, the similar stages of the radiation power decrease are observed. In this case, the first stage in both cases is characterized by saturation, which made it possible to associate its appearance with rearrangement of the initial structure of the defects. Furthermore, at the first stage, the emissive power decrease is due to identical defects and is independent of their appearance history. Similar reasoning is applicable to other determined stages. We note that the relative contribution of the stages to the overall emissive power decrease of the LEDs is defined by the type of influence.

The above-described radiation and reliability models of LEDs can be used as a basis for the development of the exploitable model of LEDs. It is a complex of relationships that describe the change in the emissive power of LEDs (criterial parameter) under the complex and combined influence of various types of ionizing radiation and long-term operation factors. The practical application of the exploitable model of LEDs will make it possible to predict the behavior of LEDs under different operating conditions. The proposed model is universal, because it describes the change in the emissive power of LEDs under the influence of damaging factors of different nature.

The physical nature of the exploitable model of the LEDs allows using it as a base for the development of exploitable models of other types of semiconductor devices.

These research results make it possible to recommend the radiation technology for improving the operational parameters of the LEDs [32, 33].

http://dx.doi.org/10.5772/intechopen.72286

4. Radiation technologies for improving reliability of the LEDs

4.1. Preliminary irradiation by gamma-quanta

Consider the influence of preliminary irradiation by gamma-quanta with further annealing of radiation-induced defects over change of emissive power during step-by-step tests.

Doses $D_{\gamma 1}$ for batch LED-4 and $D_{\gamma 2}$ for batch LED-5 were used for preliminary irradiation by gamma-quanta. The irradiation dose $D_{\gamma 1}$ corresponds to the first stage of decreasing the radiation power of the LEDs irradiated by gamma-quanta. Moreover, the dose $D_{\gamma 2}$ corresponds to the second stage of the emissive power fall of the LEDs (see **Figure 2**).

After preliminary irradiation by gamma-quanta, the annealing was carried out. Moreover, the annealing mode corresponds to the first stage of the step-by-step tests described above. **Table 1** represents the change of the emissive power after preliminary irradiation with further annealing and during step-by-step tests. Furthermore, almost complete recovery of the emissive power of the LEDs was observed to their initial values after preliminary irradiation with annealing. The measurement results were used as initial values for further research of reliability.

The use of selected preliminary irradiation doses makes it possible to obtain information about the correlation between the processes of decreasing the emissive power of the LEDs caused by the combined influence of ionizing radiation and long-term operation factors.

In the results of step-by-step tests, the LED-4 batch is very neatly divided into two distinctive subgroups LED-4a and LED-4b when the step of the tests rises.

Next, we consider obtained results in more details. **Figure 5** depicts the change of the emissive power of the LEDs from subgroup LED-4a during step-by-step tests. Furthermore, the subgroup LED-4a is divided into two subgroups LED-4a1 (20% from the batch LED-4) and LED-4a2 (35% from the batch LED-4). Moreover, **Figure 5** illustrates for comparison the change of the emissive power of the LEDs without preliminary irradiation (LED-3 batch) during operation.

Research stage	**Level of emissive power, % from initial value**							
	LED-3	**LED-4**				**LED-5**		
		LED-4a		**LED-4b**		**a**	**b**	**c**
		a1	**a2**	**b1**	**b2**			
After preliminary irradiation by gamma-quanta	—	95				8		
After annealing	—	102				97		
Initial values before step-by-step tests	100	100				100		
Before CF development	39	82	67	65	56	107	136	85
Step of the CF appearance (I_{stepi}, mA)	475	550	500	500	450	400	400	450

Table 1. The emissive power changes of the LEDs on the different stages of radiation technology implementation.

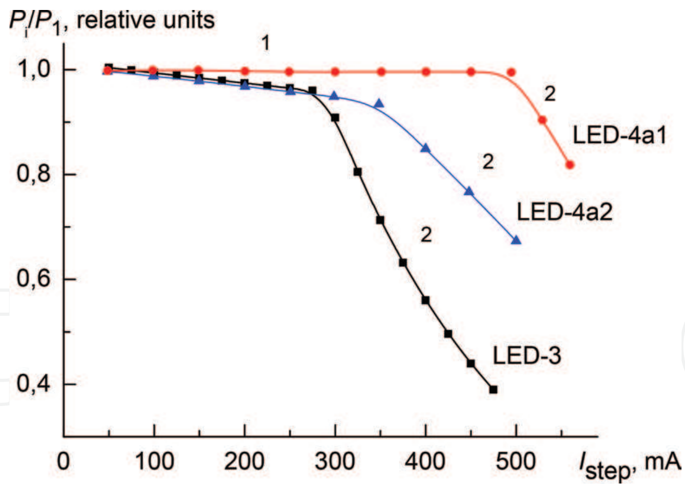

Figure 5. Relative change of emissive power of subgroup LED-4a during step-by-step tests: 1 and 2, revealed stages of the emissive power fall; LED-4a1 and LED-4a2, marked subgroups; LED-3, batch LED-3.

It is apparent that all of the presented dependences have the same form. However, the dependences differ according to the contribution of the first stage in total decrease of the emissive power of the LEDs during step-by-step tests. Therefore, **Figure 5** shows that preliminary irradiation by gamma-quanta makes it possible to decrease the contribution of the first stage (up to its complete elimination for the subgroup LED-4a1) to a total decrease of the emissive power during step-by-step tests.

Each of the marked subgroups can be characterized by the eigenvalues of the efficiency coefficient η for the LEDs after preliminary irradiation and further annealing. In this case, the efficiency coefficient means the ratio of the emission power of the LEDs to the power consumption. Here and elsewhere, the efficiency coefficient is average value for the batches and the marked subgroups. Furthermore, the change of efficiency coefficient can be described by the following equation when passing from one subgroup to other subgroups:

$$\eta_{\text{LED-3}} < \eta_{\text{LED-4a2}} < \eta_{\text{LED-4a1}} \tag{2}$$

Moreover, the dependence between emissive power fall and efficiency is absent in an explicit form for LED-3 batch.

Figure 6 represents the established dependence of the emissive power fall during step-by-step test for subgroup LED-4b. It is divided into two subgroups LED-4b1 (35% from the batch LED-4) and LED-4b2 (10% from the batch LED-4).

It can be seen that the subgroup LED-4b is divided into two subgroups, in which the change of the emissive power is determined by the corresponding value of the efficiency by the following equation:

$$\eta_{\text{LED-4b2}} < \eta_{\text{LED-4b1}} \tag{3}$$

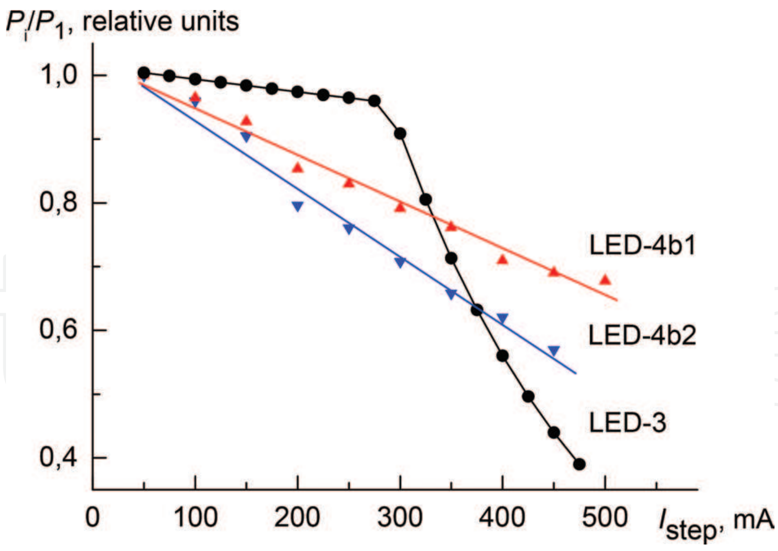

Figure 6. Relative change of the emissive power during step-by-step tests for subgroup LED-4b: LED-4b1; LED-4b2, marked subgroups; LED-3, batch LED-3.

Consequently, we obtain the following equation taking into account Eq. (3):

$$\eta_{LED-4b2} < \eta_{LED-4b1} < \eta_{LED-3} < \eta_{LED-4a2} < \eta_{LED-4a1} \tag{4}$$

Certainly, the additional research is necessary to identify the parameters that determined their specific difference for the marked subgroups of the LEDs.

In addition, the preliminary irradiation by gamma-quanta with the dose corresponding to radiation-stimulated rearrangement of the initial defect structure makes it possible to increase the resistance of ohmic contacts to the influence of long-term operation factors. Furthermore, it allows decreasing the probability of the CF development and increasing the reliability of LEDs.

Therefore, the possibility of practical application is shown to except almost completely the contribution of the first stage of decreasing the emissive power of the LEDs during step-by-step tests. It is realized by preliminary irradiation by gamma-quanta with a dose $D_{\gamma 1}$ and further annealing. This technology allows improving significantly the operational characteristics of the LEDs. The use of different levels of preliminary irradiation by gamma-quanta within the first stage (see **Figure 2**) allows controlling these processes. Furthermore, it makes possible to control the contribution of the first stage of emissive power decrease of the LEDs during operation.

Moreover, the used doses of preliminary irradiation by gamma-quanta, annealing temperature, and annealing duration are not optimal. Consequently, when the proposed radiation technology is optimized, the obtained results can exceed the values presented here.

Therefore, the preliminary irradiation by gamma-quanta with dose corresponding to the first stage of emissive power decrease of the LEDs (see **Figure 2**) with further annealing makes it possible to increase the reliability of the LEDs.

Now, turn to consider the results of step-by-step tests for batch LED-5. The LEDs of this batch were preliminary irradiated by gamma-quanta with the second dose corresponded to the second stage of the emissive power fall under irradiation by gamma-quanta (**Figure 2** and **Table 1**). We emphasize that the emissive power decrease during step-by-step tests for batch LED-5 fundamentally differs from the above-observed emissive power fall for batch LED-4. The emissive power of LEDs from the batch LED-5 (similar to batch LED-4) almost completely returns to the initial value of the emissive power after the annealing, in spite of the fact that emissive power of the LEDs decreased significantly after preliminary irradiation by gamma-quanta. This is shown in **Table 1**.

Figure 7 depicts the change of the emissive power during step-by-step tests for the batch LED-5. The batch is divided into three equal in percentage ratio subgroups (LED-5a, LED-5b, LED-5c in **Figure 7**). It should be specially noted that the observed changes of emissive power from the LED-8 batch practically do not lead to a LED failure as a result of its decrease. Moreover, the reliability of the LEDs is limited only by the development of CFs.

Two strongly marked peaks of the emissive power increase during step-by-step tests are characterized in all marked subgroups. Furthermore, some of the detected peaks clearly have a compound shape.

Each of the marked subgroups can be characterized by the eigenvalues of the efficiency coefficient for the LEDs after preliminary irradiation and further annealing. Furthermore, the change of efficiency coefficient can be described by the following equation when passing from one subgroup to other subgroups:

$$\eta_{\text{LED-5c}} < \eta_{\text{LED-5b}} < \eta_{\text{LED-5a}} \quad (5)$$

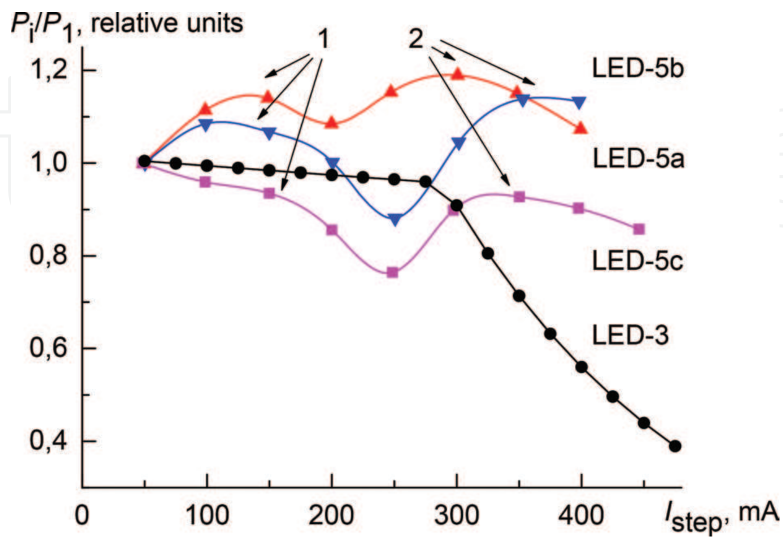

Figure 7. Relative change of the emissive power during step-by-step tests for batch LED-5: 1 and 2, recovery of the emissive power; LED-5a, LED-5b, and LED-5c, marked subgroups; LED-3, batch LED-3.

Comparing the results of the step-by-step tests for batches LED-5 and LED-3, it allows concluding that the observable annealing is probably attributed to annealing radiation defects in particular (possibly stimulated by an external electric field). The defects' precipitation is typical for the second stage of the emissive power fall of the LEDs during step-by-step tests.

The effective annealing temperatures can be estimated to the maximum of the emissive power rise using Eq. (1) for marked subgroups of batch LED-5. Therefore, the annealing of two distinctive types of defects is observed for each of marked subgroups of LED-5 batch. Moreover, the effective annealing temperature is in the range of 348–352 K for the first defect. Furthermore, the effective annealing temperature is in the range of 362–370 K for the second defect. Certainly, the effective temperatures have rough estimate that obtain in such a way. At present time, we cannot connect annealing defects with concrete types. This is subject for further research.

Analysis of the results presented in **Table 1** allows concluding that the preliminary irradiation by gamma-quanta with dose $D_{\gamma 2}$ leads to earlier appearance of CF. It is due to accelerated degradation of ohmic contacts.

Preliminary irradiation by gamma-quanta in the field of radiation defects' introduction leads to accelerated degradation of ohmic contacts and increasing the probability of CF development. Consequently, it leads to decrease the ultimate reliability of the LEDs.

The obtained results allow us to recommend the preliminary irradiation by gamma-quanta in the manufacturing technology of the LEDs to improve their operational parameters.

4.2. Preliminary irradiation by fast neutrons

Consider the influence of preliminary irradiation by fast neutrons with further annealing the radiation-induced defects over change of the emissive power of the LEDs during operation.

The change in the emissive power of the LEDs after preliminary irradiation and further annealing is presented in **Table 2**. Here, the values of the emissive power of the LEDs measured before the CF development are shown. A partial or complete recovery of the emissive power of the LEDs to the initial values is observed after annealing. These obtained results were used as initial values for further research of the reliability.

For batch LED-6, the preliminary irradiation by fast neutrons was chosen in the field of the first stage of the emissive power fall (**Figure 3**). **Figure 8** represents the change of the emissive power for batch LED-6 during step-by-step tests. Moreover, **Figure 8** illustrates the emissive power change for LED-3 batch in contrast. Furthermore, the batch LED-6 is divided into two distinctive subgroups LED-6a (55% from the batch LED-6) and LED-6b (45% from the batch LED-6).

The following equation of the efficiency can be composed for marked subgroups of the LED-9 batch:

$$\eta_{LED-6b} < \eta_{LED-3} < \eta_{LED-6a} \quad (6)$$

Research stage	Level of emissive power, % from initial value				
	LED-3	LED-6		LED-7	
		a	b	a	b
After preliminary irradiation by fast neutrons	—	95		14	
After annealing	95	111		32	
Initial values before step-by-step tests	100	100		100	
Before CF development	39	88	73	353	284
Step of the CF appearance (I_{stepi}, mA)	475	500		425	

Table 2. The emissive power changes of the LEDs on the different stages of radiation technology implementation.

Additionally, there are three distinctive peaks of the emissive power recovery for marked subgroups of the batch LED-6. The subgroups differ only in value of the emissive power recovery. The quantities of the peaks show the annealing of three types of defects. Therefore, the observable recovery of emissive power of the LEDs during operation is due to annealing of three types of the defects created by radiation-stimulated reconstruction of the initial defect structure that is stimulated by operation factors.

The effective annealing temperatures can be estimated to the maximum of the emissive power rise using Eq. (1) for marked subgroups of batch LED-6. Therefore, the annealing of three distinctive types of defects is observed for each of marked subgroups of batch LED-6. Moreover, the effective annealing temperature is in the range of 341–345 K for the first defect. Furthermore, the effective annealing temperature is in the range of 355–359 K for the second defect. Additionally, the effective annealing temperature is in the range of 369–376 K for the third defect. Certainly, the

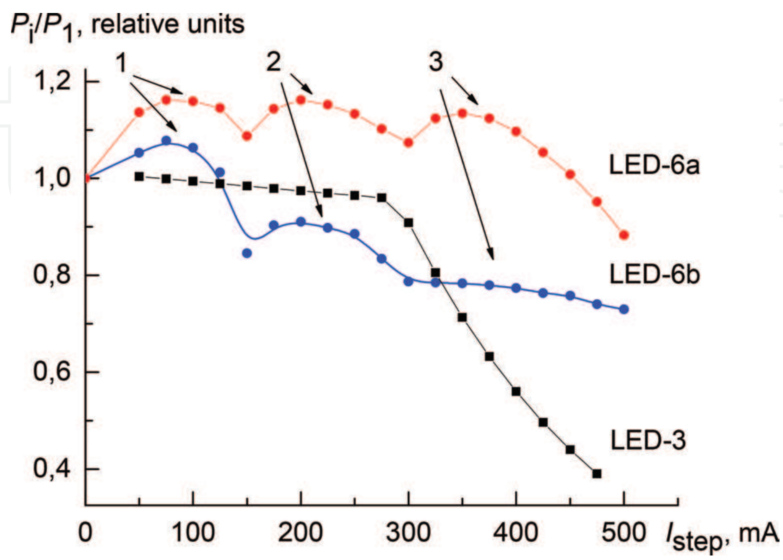

Figure 8. Relative change of the emissive power of the batch LED-6 during step-by-step tests: 1, 2, and 3, the emissive power recovery with further fall; LED-6a and LED-6b, marked subgroups; LED-3, the batch LED-3.

effective temperatures have rough estimate that obtain in such a way. At present time, we cannot connect annealing defects with concrete types. This is subject for further research. Moreover, the reliability increases for the batch LED-6 in comparison with batch LED-3.

Next, **Figure 9** shows the emissive power change of the batch LED-7 during step-by-step tests. This batch is divided into two subgroups LED-7a (70% from the batch LED-7) and LED-7b (30% from the batch LED-7).

For the marked subgroups of the LEDs from the batch LED-7, the following equation can be written as

$$\eta_{LED-7b} < \eta_{LED-7a} \tag{7}$$

There are two stages of the emissive power recovery with its further fall for subgroup LED-7a. This is due to annealing the corresponding defects. Moreover, the rate of the emissive power recovery exceeds significantly the previously observed values for batch LED-6. Therefore, the recovery of the emissive power for batch LED-7 during operation can be considered due to annealing of two types of defects. Additionally, the first of them can be attributed to the field of radiation-stimulated reconstruction of the initial defect structure under influence of the operation factors. The subgroup LED-7b is characterized by the fact that the first stage of the emissive power recovery is absent. The observed changes of emissive power are described by the measurement error. Therefore, the recovery of the emissive power for subgroup LED-7b during operation can be considered due to the annealing of the second defect only.

The effective annealing temperatures can be estimated to the maximum of the emissive power rise using Eq. (1) for marked subgroups of batch LED-7:

- Subgroup LED-7a, $T_{A1} = (360 \pm 2)$ K; $T_{A2} = (388 \pm 2)$ K.
- Subgroup LED-7b, $T_{B2} = (378 \pm 2)$ K.

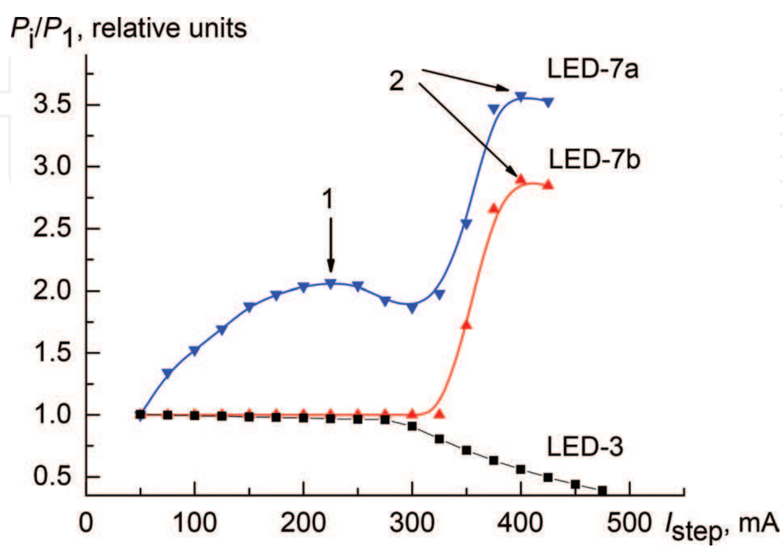

Figure 9. Relative change of the emissive power of the batch LED-7 during step-by-step tests: 1, 2, and 3, the emissive power recovery with further fall; LED-7a and LED-7b, marked subgroups; LED-3, the batch LED-3.

Consequently, the division of the initial LEDs into distinctive subgroups has been established while investigating the influence of preliminary irradiation by fast neutrons with further annealing on the operational characteristics of the LEDs. Each subgroup has its own characteristic dependence of the emissive power decrease of the LEDs during operation.

Furthermore, each subgroup can be characterized by eigenvalues of the efficiency coefficient η for the initial LEDs (after preliminary irradiation with further annealing).

Therefore, preliminary irradiation by fast neutrons makes it possible to activate the initial defect structure by decreasing its thermal resistance during further step-by-step tests.

The obtained results allow us to recommend the present radiation technology for manufacturing the LEDs. This technology is based on preliminary irradiation by fast neutrons and further annealing for improving the operational parameters of the LEDs.

5. Conclusion

The following list sums up the main investigation results of experimental studies described above:

1. The research results of the emissive power change of the LEDs based upon AlGaAs heterostructures under irradiation by gamma-quanta ^{60}Co and fast neutrons. Based on the analysis of the present results, the radiation model of the LEDs has been developed. The established laws can be used to predict the radiation resistance of the LEDs.
2. The investigation of the emissive power change of the LEDs based upon AlGaAs heterostructures during operation based on the step-by-step tests has been presented. Based on the analysis of the research, the reliability model of the LEDs has been developed. The established laws can be used to predict the reliability of the LEDs.
3. Combination of radiation model and reliability model allows to develop an exploitable model of the LEDs. This model makes possible the prediction of the change in emissive power of the LEDs under complex and combined influence of various types of the ionizing irradiation and the factors of long-term operation.
4. Radiation technology for manufacturing LEDs based upon AlGaAs heterostructures with increased radiation resistance and reliability has been presented. It bases on preliminary irradiation by gamma-quanta ^{60}Co and further annealing.
5. Radiation technology for manufacturing LEDs based upon AlGaAs heterostructures with increased radiation resistance and reliability has been developed. It depends on preliminary irradiation by fast neutrons and further annealing.
6. Decision of the optimum conditions of irradiation and annealing allows to improve significantly the radiation resistance and reliability of the LEDs based upon AlGaAs heterostructures, i.e., significantly improve their operation parameters.
7. Suggested complex of the radiation technologies can be recommended for other types of semiconductor devices.

Acknowledgements

This work was supported by the Ministry of Education and Science of the Russian Federation [grant number 03.G25.31.0224 from 03.03.2017].

Author details

Alexandr V. Gradoboev[1]*, Anastasiia V. Simonova[1], Ksenia N. Orlova[1] and Olga O. Babich[2]

*Address all correspondence to: gradoboev1@mail.ru

1 National Research Tomsk Polytechnic University, Tomsk, Russia

2 Kemerovo State University, Kemerovo, Russia

References

[1] Gradoboev AV, Surzhikov AP. The Radiation Resistance Microwave Devices Based on Gallium Arsenide. Tomsk: Tomsk Polytechnic University; 2005. 277 p

[2] Gradoboev AV, Simonova AV. Operational model of the electronic products. In: Semipalatinsk Test Site. Radiation Legacy and Development Prospects; September 21-23, 2016; Kurchatov, VKO, Republic of Kazakhstan. Pavlodar: Publishing House; 2016. p. 131-132

[3] Martin DI, Ighigeanu DI, Mateescu EN, Craciun GD, Calinescu II, Iovu HM, et al. Combined microwave and accelerated electron beam irradiation facilities for applied physics and chemistry. IEEE Transactions on Industry Applications. 2004;**40**(1):41-52. DOI: 10.1109/TIA.2003.821655

[4] Busatto G, De Luca V, Iannuzzo F, Sanseverino A, Velardi F. Single-event effects in power MOSFETs during heavy ion irradiations performed after gamma-ray degradation. IEEE Transactions on Nuclear Science. 2013;**60**(5):3793-3801. DOI: 10.1109/TNS.2013.2278038

[5] Liu C, Li X, Yang J, Ma G, Sun Z. Radiation defects and annealing study on PNP bipolar junction transistors irradiated by 3-MeV protons. IEEE Transactions on Nuclear Science. 2015;**62**(6):3381-3386. DOI: 10.1109/TNS.2015.2498201

[6] Chaffin RJ. Microwave Semiconductor Devices: Fundamentals and Radiation Effects. New York: John Wiley and Sons, Inc.; 1973. 387 p

[7] Lang DV, Petroff PM, Logan RA, Johnston Jr WD. Recombination-enhanced interactions between point defects and dislocation climb in semiconductors. Physical Review Letters. 1979;**42**(20):1353

[8] Kulakov VM, Ladygin EA. Effects of Ionizing Radiation on the Devices of Electronic Equipment. Sovetskoe Radio: Moscow, Russia; 1980. 244 p

[9] Srour JR, McGarrity JM. Radiation effects on microelectronics in space. Proceedings of the IEEE. 1988;**76**(11):1443-1469. DOI: 10.1109/5.90114

[10] Khattab K, Haddad K, Haj-Hassan H. Design of a permanent cd-shielded epithermal neutron irradiation site in the Syrian miniature neutron source reactor. Journal of Radioanalytical and Nuclear Chemistry. 2008;**277**(2):311-316. DOI: 10.1007/s10967-007-7081-7

[11] Anashin VS, Ishutin IO, Ulimov VN, Emeliyanov VV. Methods to control the hardness of specialized VLSI to space natural ionizing radiation. In: Stempkovsky A, editor. Problems of Perspective Micro- and Nanoelectronic Systems Development; October 4-8, 2010; Moscow Region. Moscow: IPPM RAS; 2010. pp. 233-236

[12] Fukuda M. Reliability testing of semiconductor optical devices. In: Ueda O, Pearton SJ, editors. Materials and Reliability Handbook for Semiconductor Optical and Electron Devices. 1st ed. New York: Springer; 2013. pp. 3-17. DOI: 10.1007/978-1-4614-4337-7_1

[13] Pecht MG, Chang MH. Failure mechanisms and reliability issues in LEDs. In: van Driel W, Fan X, editors. Solid State Lighting Reliability, Solid State Lighting Technology and Application Series. Vol. 1. New York, NY: Springer; 2013. pp. 43-110. DOI: 10.1007/978-1-4614-3067-4_3

[14] Dalapati P, Manik N, Basu A. Influence of temperature on the performance of high power AlGaInP based red light emitting diode. Optical & Quantum Electronics. 2015; **47**(5):1227-1238

[15] Alferov ZI. Nobel lecture: The double heterostructure concept and its applications in physics, electronics, and technology. Reviews of Modern Physics. 2001;**73**(3):767-782. DOI: 10.1103/RevModPhys.73.767

[16] Schubert EF, Cho J, Kim JK. Light-emitting diodes. In: Seidel A, editor. Kirk-Othmer Encyclopedia of Chemical Technology. John Wiley & Sons, Inc; 2015. pp. 1-20. DOI: 10.1002/0471238961.1209070811091908.a01.pub3

[17] Barnes CE. Effects of Co60 gamma irradiation on epitaxial GaAs laser diodes. Physical Review B. 1970;**1**(12):4735-4747. DOI: 10.1103/PhysRevB.1.4735

[18] Gromov DV, Maltcev PP, Nikiforov AY, Polevich SA, Startcev SA. Radiation hard GaAs microwave integrated circuits design. In: Radiation and Its Effects on Components and Systems, 1997. RADECS 97. Fourth European Conference on; September 15-19, 1997; Cannes, France. IEEE; 1997. pp. 147-149. DOI: 10.1109/RADECS.1997.698873

[19] Joint Stock Company "Research Institute of Devices". Research Simulator. The pulse solid-core dual-zone reactor on fast neutrons "BARS-4." [Internet]. Available from: http://www.niipriborov.ru/model_ustanov.html [Accessed: 06-07-2017]

[20] Figurov VS, Baykov VV, Shelkovnikov VV, Vasilev AV, Sushko MV. Estimation of effective spectral coefficient of neutron radiation in distant points of accelerator BARS-4 radiation

field. Questions of Atomic Science and Technics. Series: Physics of Radiation Effects on Radio-Electronic Equipment. 2011;**4**:39-51

[21] Gradoboev AV, Orlova KN, Asanov IA, Simonova AV. The fast neutron irradiation influence on the AlGaAs IR-LEDs reliability. Microelectronics Reliability. 2016;**65**:55-59. DOI: 10.1016/j.microrel.2016.07.143

[22] Gradoboev AV, Simonova AV. Influence of preliminary irradiation by gamma-quanta on development of catastrophic failures during operation of IR-LEDs. Journal of Physics: Conference Series. 2017;**830**:012132. DOI: 10.1088/1742-6596/830/1/012132

[23] Gradoboev AV, Sednev VV. Research on the radiation exposure "memory effects" in AlGaAs heterostructures. IOP Conference Series: Materials Science and Engineering. 2015; **81**(1):012007. DOI: 10.1088/1757-899X/81/1/012007

[24] Gradoboev AV, Sednev VV. The influence of power mode on IR-LED resistance to the irradiation with fast neutrons. Izvestiya Vysshikh Uchebnykh Zavedeniy. Fizika. 2014; **57**(10-3):20-23

[25] Lampert MA, Mark P. Current Injection in Solids. New York, NY: Academic Press; 1970. 363 p

[26] Gradoboev AV, Simonova AV, Orlova KN. Influence of irradiation by 60Co gamma-quanta on reliability of IR-LEDs based upon AlGaAs heterostructures. Physica Status Solidi (c). 2016;**13**(10-12):895-902. DOI: 10.1002/pssc.201600035

[27] Gradoboev AV, Orlova KN, Asanov IA. Radiation model of the LEDs based on heterostructures AlGaInP. Irradiation by gamma-quanta 60Co. In: Bondarenko GG, editor. XXII International Conference "Radiation Physics of Solid State"; July 9-14, 2012; Sevastopol. Moscow: NIIPMT-MIEM HSE; 2012. pp. 510-516

[28] Gradoboev AV, Orlova KN, Asanov IA. Irradiation of LEDs based on AlGaInP heterostructures with multiple quantum wells by 60Co gamma-rays. Perspektivnye Materialy. 2013;**7**:49-55

[29] Gradoboev AV, Orlova KN, Simonova AV. E-MRS Spring Meeting 2017, Strasbourg, France. Symposium O.7.14· Parameters changes of LEDs based on GaP under irradiation by gamma-quanta [Internet]. February 27, 2017. Available from: http://www.european-mrs.com/wide-bandgap-semiconductors-leds-solar-and-related-energy-technologies-emrs#collapse43 [Accessed: 11-07-2017]

[30] Barnes CE, Soda KJ. Application of damage constants in gamma irradiated anphoterically Si doped GaAs LEDs. IEEE Transactions on Nuclear Science. 1976;**23**(6):1664-1670. DOI: 10.1109/TNS.1976.4328559

[31] Barry AL, Houdayer AJ, Hinrichsen PF, Letourneau WG, Vincent J. The energy dependence of lifetime damage constants in GaAs LEDs for 1-500 MeV protons. IEEE Transactions on Nuclear Science. 1995;**42**(6):2104-2107. DOI: 10.1109/23.489259

[32] Gradoboev AV, Rubanov PV, Ashcheulov AV. Russian Federation Patent for an Invention no.2303314. IPC: H01 L21/18. Method for manufacturing semiconductor devices. Federal Institute of Industrial Property. Declared April 17, 2006. Published July 20, 2007; Bulletin no. 20. 6 p

[33] Gradoboev AV. Study of the "memory effect" in 3-cm band Gunn diodes under irradiation by fast neutrons. In: Microwave & Telecommunication Technology (CriMiCo), 2014 24th International Crimean Conference; September 7-13, 2014; Sevastopol, Ukraine. IEEE; 2014. pp. 870-871